



Structure-based combinatorial library design: Discovery of non-peptidic inhibitors of caspases 3 and 8

Martha S. Head^{a,*}, M. Dominic Ryan^a, Dennis Lee^b, Yanhong Feng^b, Cheryl A. Janson^c, Nestor O. Concha^c, Paul M. Keller^d & Walter E. deWolf, Jr^d

^aPhysical and Structural Chemistry, SmithKline Beecham Pharmaceuticals

^bDiscovery Chemistry US, SmithKline Beecham Pharmaceuticals

^cStructural Biology, SmithKline Beecham Pharmaceuticals

^dMechanistic Enzymology, SmithKline Beecham Pharmaceuticals, King of Prussia, PA 19406

Received 5 February 2001; Accepted 7 February 2002

Key words: caspase 3, caspase 8, inhibitors, structure-based design, combinatorial library

Summary

Structure-based design of a combinatorial array was carried out in order to identify non-peptidic thiomethylketone inhibitors of caspases 3 and 8. Five compounds from the designed array were active against caspase 3, and two were active against caspase 8. A 2.5-Å resolution co-crystal structure of caspase 3 and a thiomethylketone array member is reported. The structure-based design strategy has proved useful for identifying caspase inhibitors.

Introduction

Many biological processes such as cellular development and tissue homeostasis are regulated by apoptosis, a mechanism of cell death distinct from necrosis. In contrast to necrosis, which is a passive process caused by acute cell injury, apoptosis is an active process characterized by a well ordered series of events. A balance between promotion and inhibition of apoptosis ensures a complex regulation between cell death and proliferation under normal conditions. Conversely, an imbalance can lead to pathological states such as cancer and autoimmune disease or to damage arising from stroke or cardiac injury [1, 2, 3].

Some members of the caspase family of cysteine proteases play a key role in the initiation and regulation of apoptosis [4, 5]. To date, at least twelve caspases have been identified based on homology to known caspases such as caspase 1/ICE [3]. Furthermore, X-ray crystallographic structures are available for several caspases [6, 7, 8, 9, 10]. Because of the availability of structural data and because of their

likely role in disease states caused by dysregulated apoptosis, members of the caspase family are attractive targets for structure-based design of therapeutic agents.

Previous efforts identified isatins as a potent and selective class of inhibitors of caspase 3, *e.g.* compound **A** (Figure 1) which exhibited K_i s of 15 and 4900 nM *versus* caspases 3 and 8, respectively [10, 11]. However, inhibitors chemically distinct from isatins were also desired. Therefore, a structure-based design effort was initiated. The structure-based approach allowed the opportunity to look not just at caspase 3 but also at its homolog caspase 8, while still drawing on the extensive experience gained in the isatin series.

A number of chemical classes have been identified as inhibitors of cysteine proteases [12]. Members of the thiomethylketone class, exemplified generically by template **B** (Figure 2), have been reported as inhibitors of caspase 1/ICE [13, 14]. In addition, the thiomethylketone class of inhibitors have lower electrophilicity relative to isatins or aldehydes and were therefore judged to have lower potential for toxicity.

*To whom correspondence should be addressed: E-mail: Martha_S_Head@sbphrd.com

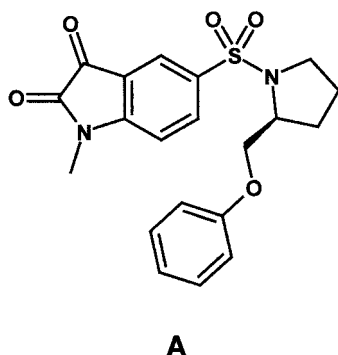


Figure 1. Isatin inhibitor of caspase 3.

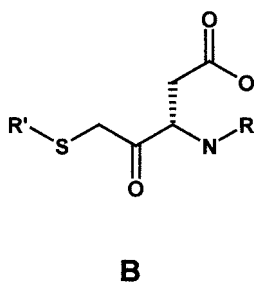


Figure 2. Thiomethylketone array template.

Thus this template was selected as a starting point for structure-based design.

Results and discussion

Library Design

A combinatorial array was designed for thiomethylketone template **B** using a crystal structure of caspase 3 and an homology model of caspase 8. The thiomethylketone was postulated to bind to the caspases through a covalent attachment of the carbon of the activated ketone to the sulfur of the catalytic cysteine. This covalent attachment is an important constraint on the system which drove the selection of QXP [15] as the docking method of choice. In work with the isatin series of caspase inhibitors, the use of QXP was validated by the ability to correctly predict the covalently bound binding mode of isatin **A** to caspase 3. An additional benefit of the QXP methodology was the ability to automatically link a set of reagents to a chemical template, enabling a straight-forward process for virtual screening of the combinatorial array.

The design goal was to identify functional groups that would bind in the unprime side of the active site.

Therefore, a relatively small set of R' groups was selected on the basis of availability and ease of synthesis. The eight selected R' groups are listed in the first row of Table 1. Structural data guided the selection of reagents for the unprime side of the thiomethylketone template using an automated docking procedure.

Virtual reagent list. Possible reagents for the unprime side of template **B** were selected from the Available Chemicals Database (ACD). Monoacids with molecular weight less than 500 were selected. The list of possible reagents was further filtered to remove compounds with more than one peptide bond and more than four consecutive rotatable bonds. This process resulted in a list of approximately 7,000 monoacids for use in computational screening.

Automated combinatorial docking. To identify the initial template locations within the protein active sites, a simplified thiomethylketone (R and R' of template **B** set to methyl) was docked into the caspase 3 (Figure 3a) and caspase 8 (Figure 3b) structures. The template location in both caspase 3 and 8 placed the carboxylic acid of the template into the S1 binding sub-site. However, a difference in template docking was seen in the two enzymes for the location and orientation of the connection point for subsequent computational reagent screening (Figure 3).

Automated virtual screening calculations were then carried out in which each of the 7,000 monoacid reagents was computationally linked to the template connection point, shown in cyan in Figure 3. For each of the calculations, the substituent was conformationally searched in the presence of the protein. The template was flexible in that it could adjust to the position of the substituent, but was not conformationally searched during this phase of the calculation. The best-scoring position for each substituent was retained. Each virtual compound was docked and scored twice, once for caspase 3 and once for caspase 8.

Reagent selection. Docking results were filtered to obtain two virtual libraries, one directed at caspase 3 and one at caspase 8. The process is outlined in Figure 4. Three criteria were used to obtain the final selections of R reagents. First, the virtual screening results were filtered on the basis of docking scores to remove substituents that were not compatible with the protein structures. Second, distance filters were used to assess interactions with the S2 pockets of the binding sites. This filter was selected on the basis our

Table 1. Initial results for screening of the thiomethylketone array^a.

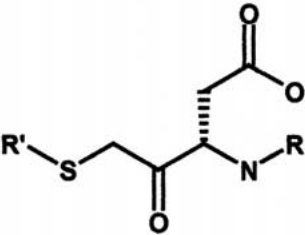
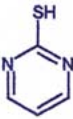

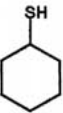
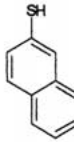
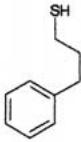
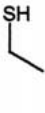
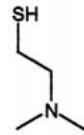
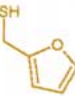
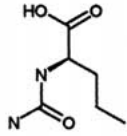
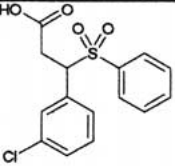
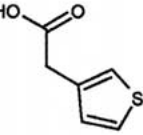
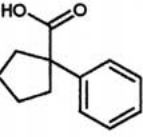
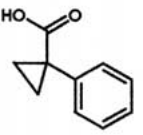
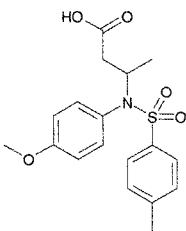
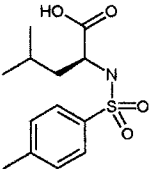
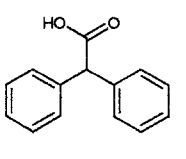
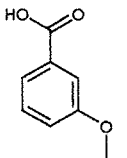
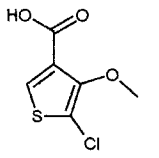
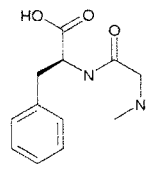
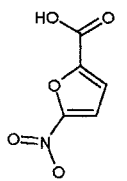
								
R'								
R								
	—	—	—	—	I ^b I	—	—	—
	I I	I I	I I	I I	I I	I I	I I	—
	I I	I I	I I	I I	I I	I I	—	—
	I I	I I	I I	I I	I I	I I	—	—
	I I	I I	—	I I	I I	I I	I I	—

Table 1. Continued.

	93%	I	I	I	I	I	I	—
	I	I	I	I	I	I	I	—
	60%	31% ^c	I	I	I	I	I	—
	92%	I	I	I	I	I	I	—
	I	69%	I	I	I	I	I	—
	I	I	I	I	I	I	I	—
	58%	I	I	I	I	I	I	—
	I	I	I	I	I	I	I	—
	I	I	I	I	I	I	I	—
	63%	I	I	I	I	I	I	—
	—	—	—	—	—	—	—	—
	—	—	—	—	—	—	—	—

^a Percent inhibition measured at 25 μ M *versus* caspases 3 (upper values) and 8 (lower values)

^b Inactive: showed no appreciable inhibition at 25 μ M

^c Percent inhibition measured at 5 μ M

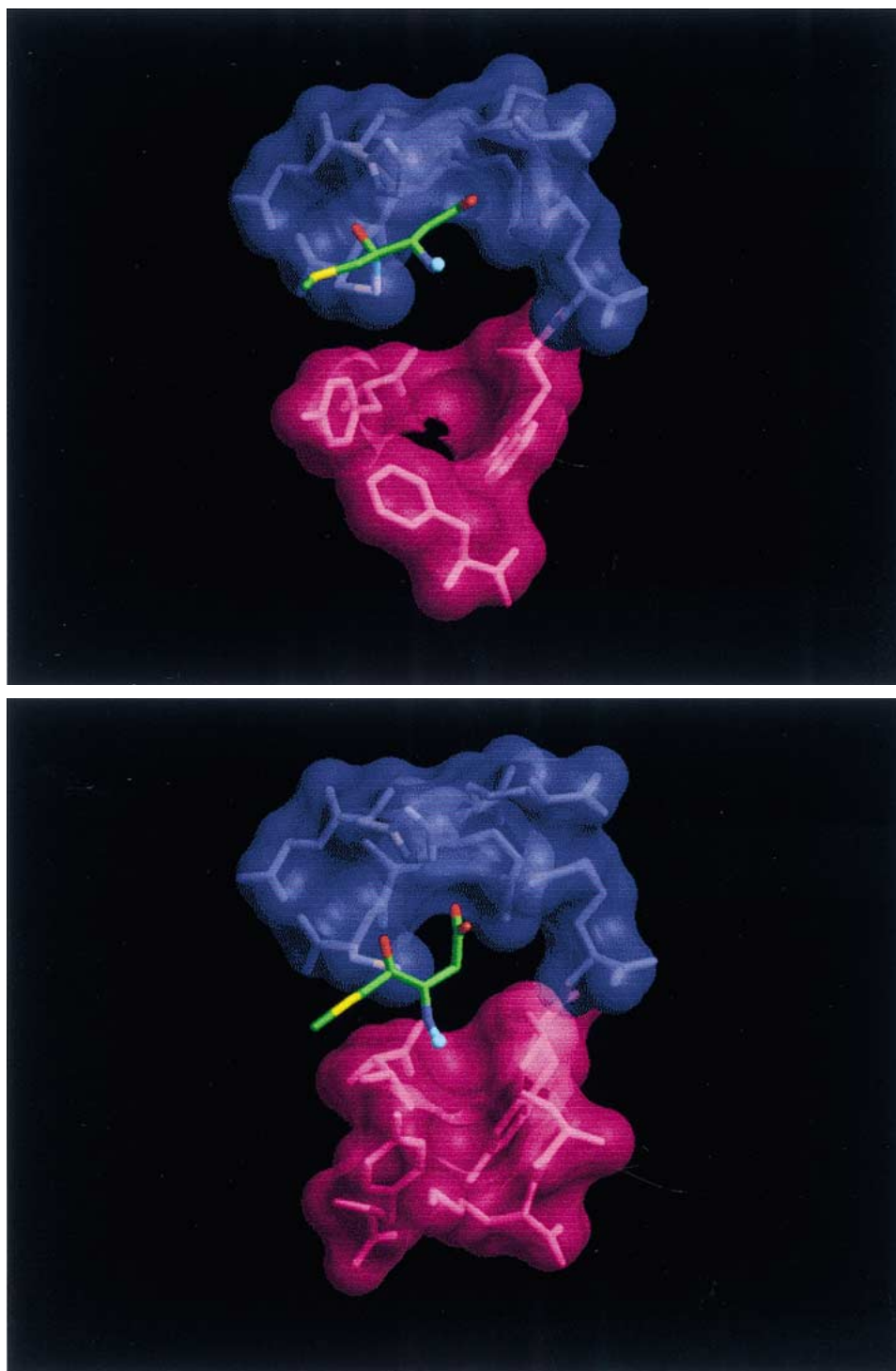


Figure 3. Thiomethylketone template docked into (a) caspase 3 and (b) caspase 8. Figures were created using the program MolMol (Koradi et al., 1996).

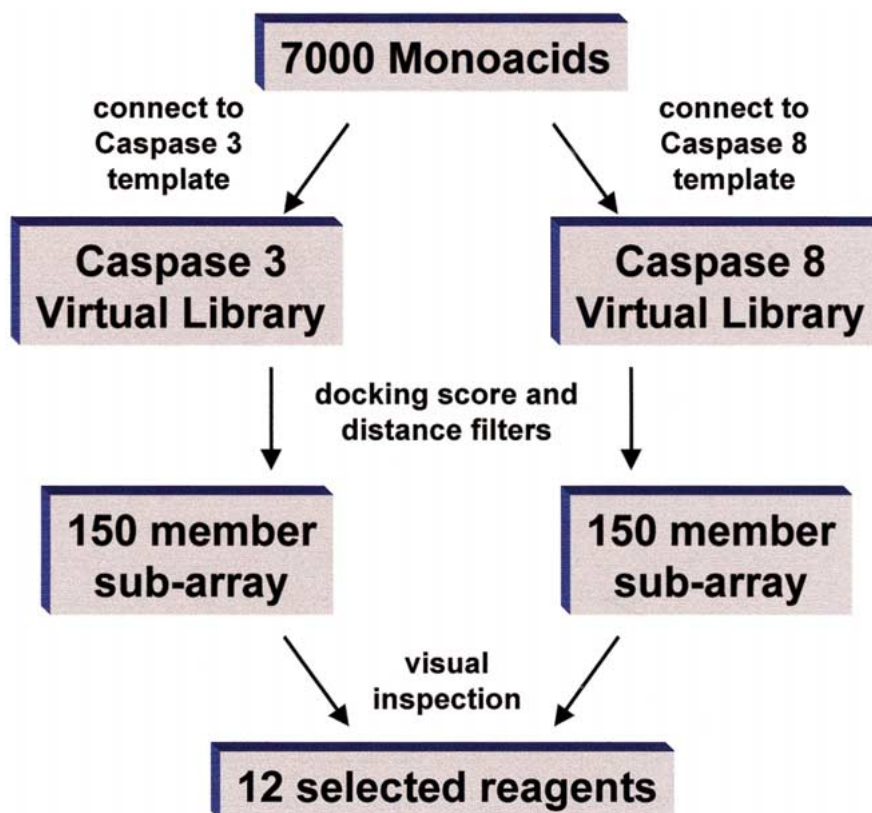


Figure 4. Reagent selection process.

knowledge of isatin SAR and crystal structures, suggesting that interacting with the S2 pocket provides affinity and selectivity [10]. The distance criteria were different for the two caspases, due to the facts that the thiomethylketone template docks differently in the two caspase structures and that the S2 sub-sites of the two caspases differ significantly. Because of these structural differences between the two caspases, a divergence was expected for the results of the virtual screening and array design process.

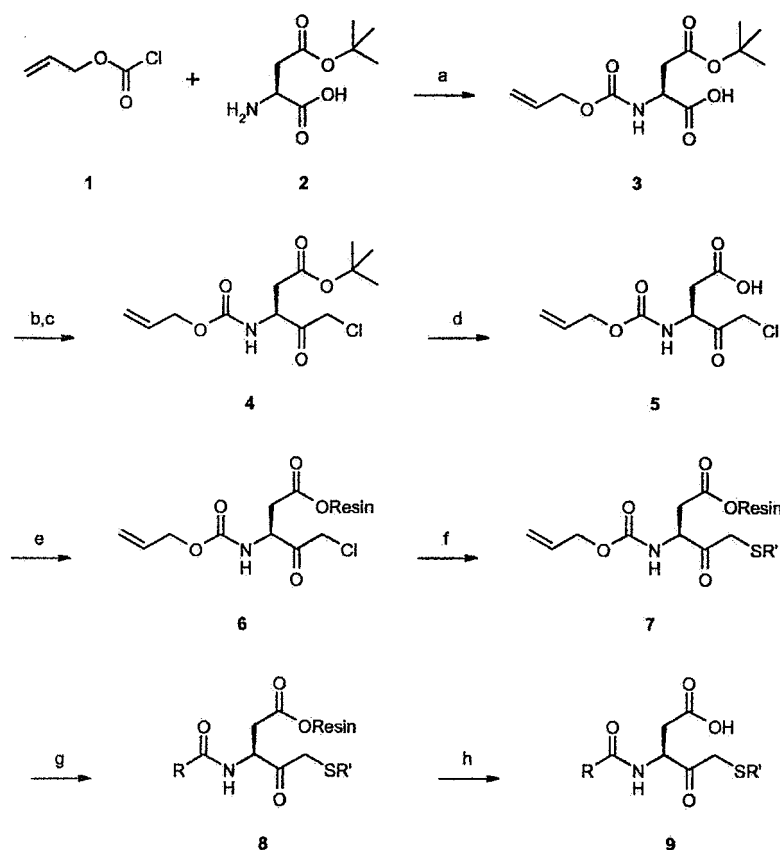
For each protein, approximately 150 reagents passed the score and distance filters. As expected, there was only small overlap between the lists of filtered reagents for each structure. Approximately 10% of these reagents underwent full conformational sampling in order to validate the binding modes produced by the automated docking calculation. The results obtained by full conformational sampling were consistent with the virtual screening docking modes.

To complete a 96 member array, twelve R-group reagents had to be selected for the synthesis. Thus the final filter applied was a visual inspection of predicted

binding modes. The twelve selected R group reagents are listed in the first column of Table 1. Seven of the twelve reagents were selected for caspase 3 (rows 1–7 of Table 1), three were selected for caspase 8 (rows 10–12), and two were compatible with both caspase structures (rows 8 and 9). A number of sulfonamides were in the set of reagents which passed the score and distance filters for caspase 3; a subset of these were included to explore possible similarities to the isatin series. Other reagents were chosen with a bias towards small size and a predicted binding mode which would allow for later elaboration of any hits from the array. Specifically, virtual array components were selected which accessed only the S1 and S2 binding subsites. The eight R' groups to complete the array were not selected computationally, but were selected on the basis of availability, diversity, and ease of synthesis.

Chemistry

Aspartic acid *tert*-butyl ester **2** was treated with allyloxycarbonyl chloride **1** to produce N-allyloxycarbonyl-aspartic acid **3** (Scheme 1). N-Allyloxycarbonyl-



Scheme 1 Solid-phase Synthesis of an Array of Thiomethylketones

a: Na_2CO_3 ; b: EtOCOCl , NMM, CH_2N_2 ; c: HCl in ether; d: TFA , CH_2Cl_2 ; e: Ph_3P , DEAD, THF, Wang Resin; f: R_2SH , DIEA, CH_2Cl_2 ; g: $\text{R}_1\text{CO}_2\text{H}$, EDC, HOBT, Bu_3SnH , $\text{Pd}(\text{Ph}_3\text{P})_4$, DMF, CH_2Cl_2 ; h: 2.5% TIS in 1:1 $\text{TFA}:\text{CH}_2\text{Cl}_2$

aspartic acid **3** was converted to chloromethylketone **4** by treatment with ethylchloroformate and N-methylmorpholine in THF, followed by treatment with diazomethane, and quenching with HCl in ether. *tert*-Butyl ester **4** was converted to carboxylic acid **5** with trifluoroacetic acid in CH_2Cl_2 , then was attached to Wang resin using the Mitsunobu reaction [16]. The chloride was displaced with a variety of mercaptans in Hunig's base to afford thiomethylketones **7**. Thiomethylketones **7** were deprotected *in situ* using tributyltin hydride and *tetrakis*(triphenylphosphine)palladium(0) [17]. Various carboxylic acids were coupled to the resulting amines using EDC and HOBT [18], providing intermediate amides **8**. Cleavage from the Wang-polystyrene beads was accomplished by treatment with triisopropylsilane and trifluoroacetic acid in methylene chloride to give the final array thiomethylketones **9**. Sixty-one components out of a targeted ninety-six were successfully prepared, as characterized by mass spectrometry and proton NMR.

Table 2. Activities of selected compounds from array.

Compound	Caspase 3 IC_{50}^a μM	Caspase 8 IC_{50}^a μM
C	6 ± 2	I ^b
D	9 ± 1	I
E	18 ± 4	I
F	21 ± 5	I
G	37 ± 16	2.7 ± 0.6
H	I	7.3 ± 0.9

^aEstimates of the standard errors are for a single IC_{50} determination.

^bNo inhibitory activity at 25 μM .

Enzymology

Caspase 3 screening. The sixty-one successfully synthesized array components were assayed against caspase 3 at a concentration of 25 μM . Five of the

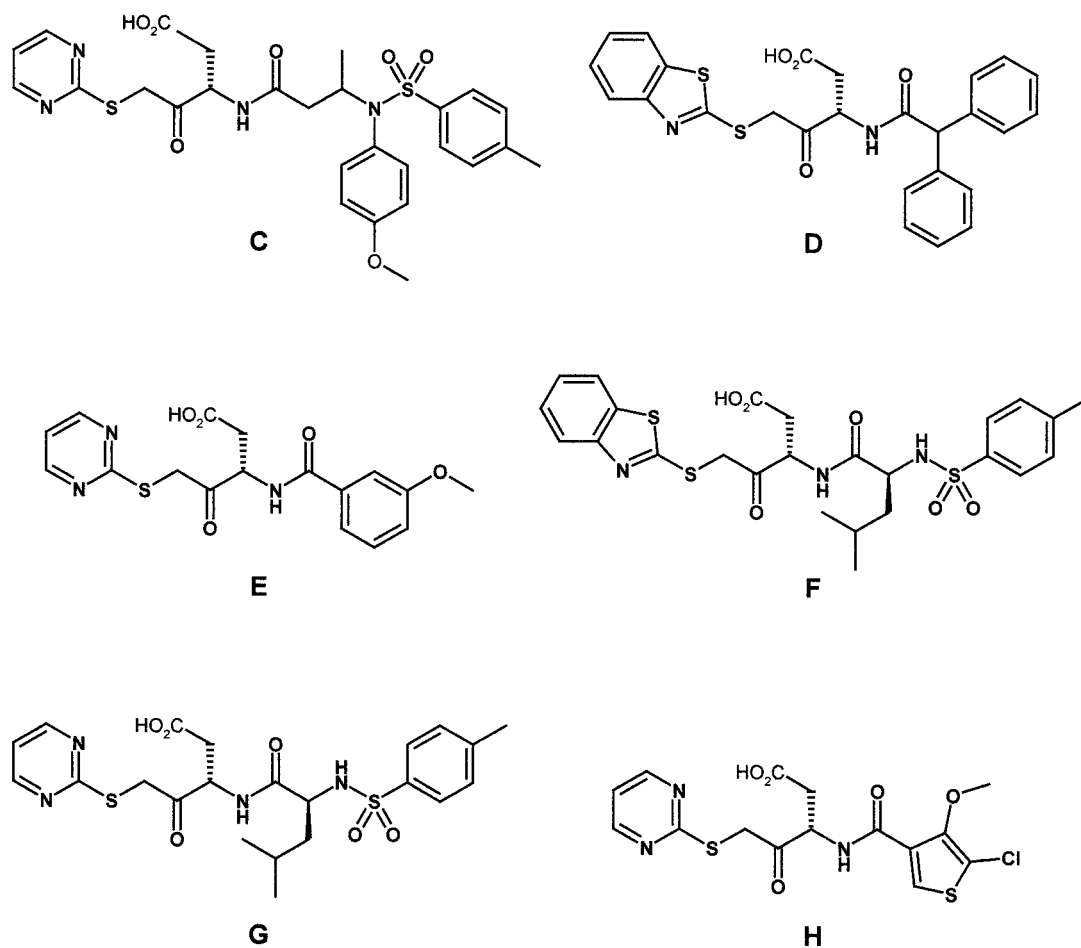


Figure 5. Array components which showed activity against caspases 3 and 8.

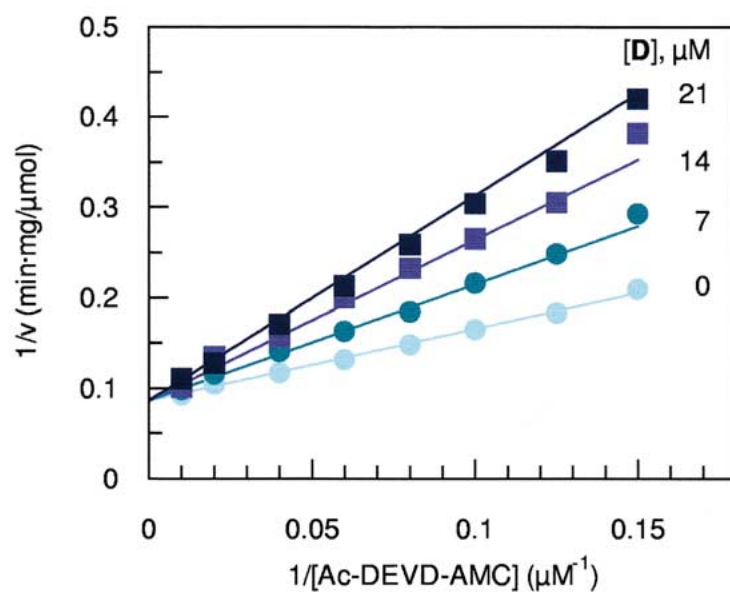


Figure 6. Kinetic data for inhibition of caspase 3 by thiomethylketone **D**.

array components – compounds **C–G** – were active (Figure 5). The IC_{50} values determined for these five compounds *versus* caspase 3 ranged from 6–37 μ M (Table 2). Inhibition profiles were determined for each compound by estimating the initial velocities (i.e., the slope of the tangent to the progress curve at $t = 0$) at different concentrations of substrate and inhibitor. Under these conditions, which factor out any time-dependent effects on the inhibition, all five compounds were shown to be competitive *versus* substrate (data not shown). Representative kinetic data for compound **D** is shown in Figure 6, having a measured K_i value of 11 ± 1 μ M. While this value is somewhat higher (approximately two-fold) than expected based on its IC_{50} of 9 μ M (Table 2), variability of this magnitude within a screening environment is normal and usually considered insignificant.

Caspase 3 mechanistic studies. Isatin **A** and thiomethylketones **C** and **D** were examined for reversibility of inhibition. Compounds were pre-incubated with caspase 3 for 2 h to achieve maximal enzyme inhibition, followed by dilution into buffer and assay for recovery of activity over 2.5 h. The isatin inhibitors bind covalently to caspase 3, but are freely and rapidly reversible [10, 11]. As shown in Figure 7, after pre-incubation with isatin **A** the enzyme immediately regained all activity upon dilution, consistent with rapid, reversible inhibition of caspase 3. Conversely, enzyme incubated with thiomethylketones **C** and **D** did not recover activity after dilution for 2.5 h, suggesting that both compounds are irreversible inhibitors of caspase 3.

Caspase 8 screening. The sixty-one successfully synthesized array components were assayed against caspase 8. Two of the array components – compounds **G** and **H** – were active (Figure 5). IC_{50} values of approximately 3 and 7 μ M were determined for these two caspase 8 hits (Table 2).

Crystallography

A 2.5-Å resolution X-ray crystal structure of the complex between caspase 3 and thiomethylketone **D** was obtained. Data collection and refinement statistics are given in Table 3. A schematic of the bound conformation of thiomethylketone **D** is shown in Figure 8. The sulfur of catalytic cysteine 279 is linked to C*, alpha to the activated ketone, with the carbonyl oxygen occupying the ‘oxyanion hole’ and interacting with the

Table 3. Crystal Structure Data.

Data collection statistics	
Resolution	50–2.5 Å
Redundancy	5.5
R_{sym}	0.090
Completeness	96.4%
$\langle I \rangle / \sigma \langle I \rangle$	6.6
Refinement statistics	
R	0.19
R_{free}	0.26
RMS bond lengths	0.01 Å
RMS bond angles	1.5°
Reflections (R_{free})	10,0007 (993)
Protein atoms	1882
Solvent atoms	50
Inhibitor atoms	24

main chain amide nitrogens of Gly 238 and Cys 279. (Residue numbers are numbered relative to caspase 1/ICE, as in structure 1pau [6].) The aspartate side chain is bound in the S1 pocket in much the same way as the aspartate side chain of peptide inhibitors. One of the phenyl rings is bound in the hydrophobic S2 pocket formed by Tyr338, Trp340, and Phe380H. The second phenyl ring is bound along the active site and follows the trace of the main chain of the peptide inhibitors. No atom in **D** interacts with amino acids forming the P3 or P4 sites. No electron density is seen for the benzothiazole or the sulfur of the thioether. This crystal structure is consistent with the mechanistic data showing that thiomethylketone **D** binds irreversibly to caspase 3.

Comparison of predicted and observed results

While the design of a structure-based library for these enzymes was based on the hypothesis of a reversible thiohemiketal, the hits in the array were bimodal inhibitors that bound reversibly to the enzyme, followed by conversion to an irreversible attachment to the catalytic cysteine. The experimental results can be analyzed in light of the observed *versus* predicted covalent attachment point on the ligand. Success of the caspase array design strategy can be assessed by the overall results in terms of compound activities and by the accuracy of the protein-ligand binding predictions.

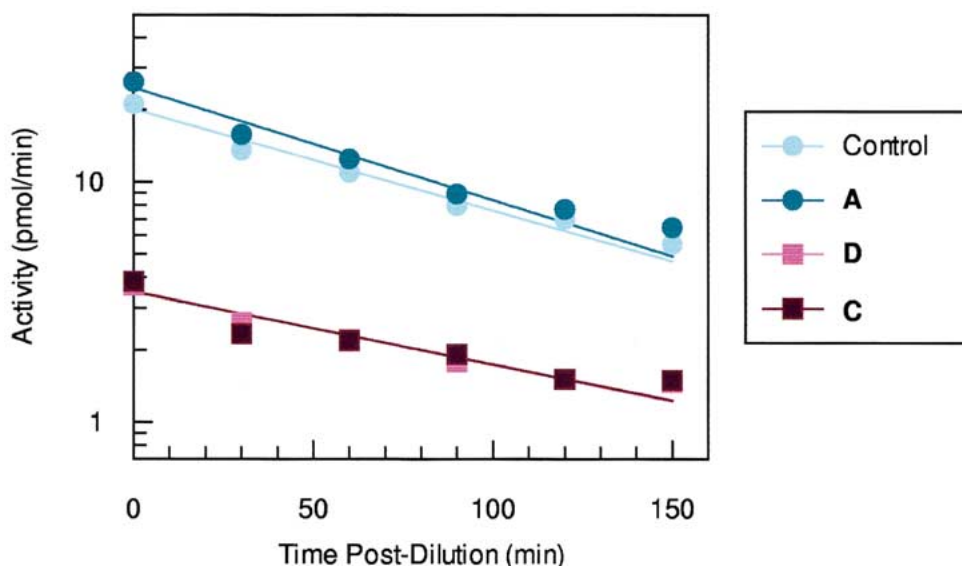


Figure 7. Mechanistic data examining irreversibility of binding of isatin **A** and thiomethylketones **C** and **D**.

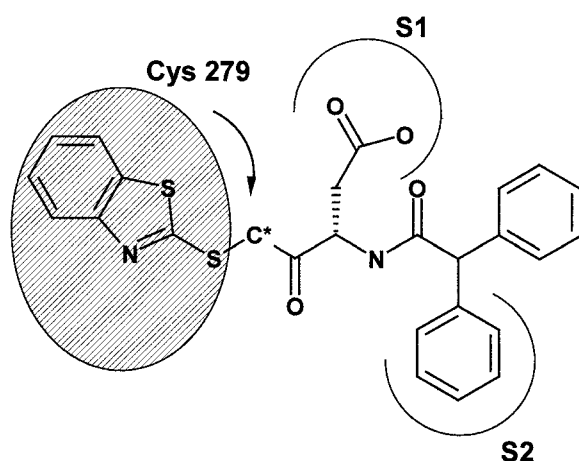


Figure 8. Crystallographically determined interactions of thiomethylketone **D** with caspase 3 binding site.

Enzymology. The observed compound activities are consistent with bimodal inhibition as described by Brady et al. [14, 19]. The first step of the inhibition process is formation of a thiohemiketal as modeled. The kinetic data and IC_{50} s reported in Figure 6 and Table 2 characterize this reversible phase. The second step of the process involves rearrangement of the thiohemiketal intermediate to an α -thiomethylketone, with loss of the R' thiol group. The lack of activity upon dilution shown in Figure 7 is consistent with this bimodal mechanism.

Array activity profile. The irreversible product complex arises through the elimination of an aromatic thiol leaving group. Examination of the reagents selected for the unprime side suggests a clear distinction in activity for the better leaving groups. One would not expect this mechanism of interaction to be operational with poorer leaving groups on the unprime side of the molecule. Thus, of the successfully synthesized array components, only the compounds listed in columns 1 and 2 of Table 1 could be expected to show activity against caspases 3 and 8. Of these eighteen compounds, six show activity, a proportion suggesting that structure-based elements of the design were in fact correct. Of the five compounds which showed caspase 3 activity, all were selected specifically for caspase 3. Similarly, the compound which has only caspase 8 activity was selected for caspase 8. A perfect prediction would have been if compound **D** rather than compound **G** had shown caspase 8 activity. The fact that compounds are active against the targeted caspase suggests that the reversible-intermediate design strategy captured key elements governing binding of the compounds to the enzyme.

IC_{50} values, a measure of the reversible component of bimodal inhibition, are consistent with modeling based on a tetrahedral intermediate. Nanomolar activities were not expected based on the reduced electrophilicity of the thiomethylketone template relative to isatins or aldehydes and on the S1'-S2 restriction on the size of the designed molecules. Greater potency

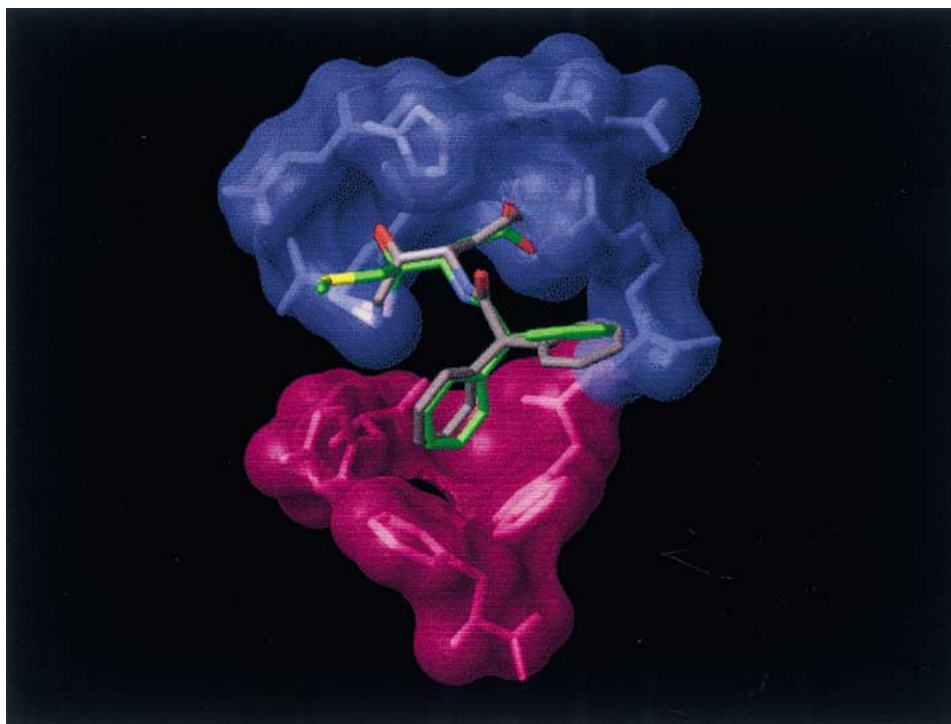


Figure 9. Co-crystal structure of **D**:caspase 3 (carbons shown in gray) compared to predicted binding mode (carbons shown in green).

could in principle be obtained by elaboration of the leads to access the S3 and S4 binding subsites.

Binding mode prediction in Caspase 3. Structurally, the crystallographic data support the design strategy based on a tetrahedral intermediate. As seen in Figure 9, with the exception of the covalent attachment point, the binding mode for compound **D** was well-predicted. One might expect that the observed mode of attachment could lead to substantial shift of the R substituent relative to a prediction based on covalent attachment to the carbonyl carbon. Interestingly, this rearrangement did not dominate the determination of binding mode. Instead, the placement of the acid substituent in S1 and of the ketone oxygen in the oxyanion hole appears to drive the binding conformation of the thiomethylketone template, with the side chain of the catalytic cysteine shifting to accommodate the observed covalent attachment upon conversion to the irreversible final product.

A question that arises is whether modeling the observed covalent attachment point (C^* , Figure 8) would have led to selection of the same set of R groups. In order to address this question, docking calculations were carried out in which the catalytic

cysteine of caspases 3 and 8 was attached to C^* of the thiomethylketone template. With the exception of minor perturbations of the cysteine sulfur and C8 positions, the binding modes predicted are virtually identical to those predicted when the template is attached through the carbonyl carbon. These results suggest that the structure-based aspects of the design directly influenced the activity profile of the array.

Conclusions

Despite the difference between the modeled and crystallographically determined attachment mode of the thiomethylketone template to caspase 3, the structure-based design strategy described herein has proved effective for producing leads against caspases 3 and 8. The design strategy identified small compounds of moderate affinity which could in future be elaborated to achieve greater potency. Moreover, comparison of the predicted binding modes for the postulated *versus* observed covalent attachment suggest that the mode of attachment plays a small role in the orientation of these ligands in the binding site. This study supports the use of structure-based technology for the design of caspase inhibitors.

Experimental methodology

Molecular modeling

Caspase 3 structure preparation. A publicly available co-crystal structure with DEVD-aldehyde (PDB code 1pau [6]) was used for virtual screening calculations in caspase 3. The DEVD-aldehyde inhibitor was removed from the structure, and polar hydrogens were added and minimized using CHARMM through the Quanta interface (MSI, San Diego California).

Caspase 8 homology model. A caspase 8 homology model was built using the Modeler module of Quanta (MSI, San Diego California), with caspase 3 crystal structure 1pau as the structural template.

Library docking and design. All docking calculations, for both template placement and automated virtual library screening, were carried out using the program QXP [15]. In the case of caspase 3 virtual screening, all protein atoms in the active site were fixed throughout the calculations, with the exception of Tyr338, Trp340, and Phe380H in the S2 sub-site. These three residues were constrained to their crystallographic conformations. In the case of virtual screening against the caspase 8 homology model, all amino acids lining the binding site were fully flexible throughout the calculations.

To determine template placement, a covalent interaction was formed between the carbon of the template ketone carbonyl and the catalytic cysteine sulfur of caspase 3 or 8. The template in each protein active site then underwent 500 cycles of Monte Carlo docking. The best-scoring docking mode was chosen as the template starting point for further calculations.

For screening of the virtual array, monoacids were sequentially attached to the thiomethylketone template. Each resulting virtual library member underwent 25 cycles of Monte Carlo docking, and the best-scoring docking mode was stored for later examination. During the Monte Carlo docking, atoms of the attached monoacid were fully searched. Atoms of the template were not searched, but were allowed to minimize to accommodate the positioning of the substituent. A small number of virtual library members underwent 500 cycles of Monte Carlo docking, with all atoms of the thiomethylketone template and the attached substituent fully searched.

For use as a filter for docking results, a pseudo-distance d was computed for each virtual library member according to Equation 1:

$$d = \left\{ \frac{\sum_{i=1}^M \sum_{j=1}^N |(R_i - R_j)|^2}{M \cdot N} \right\}^{1/2} \quad (1)$$

where M is the number of atoms in selected amino acid side chains, N is the number of atoms in the substituent attached to the thiomethylketone template, and R_i and R_j are the coordinates of each of these atoms. For caspase 3, the side chain atoms of Tyr338, Trp340, and Phe380H were used in this computation. For caspase 8, the side chain atoms of Tyr143, Pro193, and Lys234 were used.

Protein supply and enzyme inhibition assays

Recombinant full length human caspases 3 and 8 were expressed and purified as previously described [10]. Enzyme assays were run in 200- μ l volumes and contained the following: 25 mM K^+ HEPES buffer, pH 7.5, 0.1% CHAPS, 50 mM KCl, 5 mM β -mercaptoethanol, and 10 μ M Ac-DEVD-AMC (caspase 3); or Na^+ MOPS, pH 7.5, 10% glycerol, 0.25 mM EDTA, 5 mM β -mercaptoethanol, and 10 μ M Ac-IETD-AMC (caspase 8). Recombinant caspases were diluted into the appropriate buffer to about 10 U/assay (1 U = 1 pmol of AMC product formed per minute) and were added to the above incubation mixtures. All inhibitors from the array were dissolved into DMSO prior to addition to the assay mixture and tested at a concentration of 25 μ M; the final DMSO concentration was 5%. Accumulation of AMC was measured at 30 °C with a Cytofluor 4000 fluorescent plate reader (Perseptive Biosystems) at excitation/emission wavelengths of 360 nm/460 nm.

Mechanistic studies

The inhibition profiles for compounds from the array were determined for caspase 3 using buffer conditions as described above. The concentration of Ac-DEVD-AMC was varied from 6.67–100 μ M, and the inhibitor concentration was varied from 0–21 μ M. Initial velocities were fit using GraFit 4.0 (Erithacus Software,

*Abbreviations: HEPES – N-[2-hydroxyethyl]piperazine-N'-[2-ethansulfonic acid]; CHAPS – 3-[(3-cholamidopropyl)dimethylammonio]-1]propanesulfonate; MOPS – 3-[N-morpholino]propanesulfonic acid; AMC – 7-amino-4-methylcoumarin; Ac-DEVD-AMC – Acetyl-Asp-Glu-Val-Asp-AMC; Ac-IETD-AMC – Acetyl-Ile-Glu-Thr-Asp-AMC

Staines, U.K.) to Equation 2 describing linear competitive inhibition [20]:

$$v = \frac{V_m S}{K_m(1 + \frac{I}{K_i}) + S} \quad (2)$$

where v is the observed velocity, S is the substrate concentration, V_m is the velocity at saturating substrate, K_m is the Michaelis constant of the substrate, I is the inhibitor concentration, and K_i is the dissociation constant of the inhibitor from the E-I complex.

Compounds **A**, **C**, and **D** were tested for reversibility. Each compound was preincubated with caspase 3 at twice the IC_{50} concentration for two hours at 22–23° to achieve equilibrium. Under these conditions, caspase 3 activity was completely inhibited. The preincubation mixture was then diluted fifty-fold into standard assay buffer and distributed as six aliquots into an assay plate. Substrate was added at 30-min intervals after dilution to monitor the recovery of enzymatic activity.

Structure determination and refinement

The caspase 3:thiomethylketone complex was co-crystallized from 14–18% PEG2000, 0.1 M Bis-TRIS propane buffer, pH 7.0, 20 mM DTT. The co-crystals of caspase-3 with the inhibitor belong to space group $P2_12_12$ with unit cell dimensions $a = 96.4 \text{ \AA}$, $b = 68.8 \text{ \AA}$, $c = 43.4 \text{ \AA}$, and one molecule in the asymmetric unit. Diffraction data was collected at beamline X25, NSLS. The data is 96.4% complete to 2.5 \AA with $R_{\text{sym}} = 0.090$. The molecular replacement solution had a correlation coefficient of 0.608 and an R -factor of 0.363. The model was refined by minimizing the maximum likelihood target implemented in the program CNS against all data to 2.5 \AA resolution. The final R_{free} is 0.26 and R -factor is 0.19. The model includes residues 150 to 289 of p17, and 320 to 411 of p12, one inhibitor molecule, and 50 solvent molecules.

References

- Nuttall, M.E., Levy, M.A., James, M.F., and Winkler, J.D., *Emerging Drugs*, 3v (1998) 317.
- Thornberry, N.A. and Lazebnik, Y., *Science*, 281v (1998) 1312.
- Talanian, R.V., Brady, K.D., and Cryns, V.L., *J. Med. Chem.*, 43(18), (2000) 3351.
- Kaufmann, S.H. (ed.), *Apoptosis: Pharmacological Implications and Therapeutic Opportunities*. Academic Press, San Diego, CA, (1997).
- Lockshin, R.A., Zakeri, Z., and Tilly, J.L. (eds.), *When Cells Die*. Wiley-Liss, New York, (1998).
- Rotonda, J., Nicholson, D.W., Fazil, K.M., Gallant, M., Gareau, Y., Labelle, M., Peteron, E.P., Rasper, D.M., Ruel, R., Vaillancourt, J.P., Thornberry, N.A., and Becker, J.W., *Nature Struct. Biol.*, 3, (1996) 619.
- Rano, T.A., Timkey, T., Peterson, E.P., Rotonda, J., Nicholson, D.W., Becker, J.W., Chapman, K.T., and Thornberry, N.A., *Chem. Biol.*, 4, (1997) 149.
- Mittl, P.R.E., Di Marco, S., Krebs, J.F., Bai, X., Karanewsky, D.S., Priestle, J.P., Tomaselli, K.J., and Gruetter, M.G., *J. Biol. Chem.*, 272 (1997) 6539.
- Okamoto, Y., Anan, H.K., Nakai, E., Morihira, K., Yonetoku, Y., Kurihara, H., Sakashita, H., Terai, Y., Takeuchi, M., Shibamura, T., and Isomura, Y., *Chem. Pharm. Bull.*, 47, (1999) 11.
- Lee, D., Long, S.A., Adams, J.L., Chan, G., Vaidya, K.S., Francis, T.A., Kikly, K., Winkler, J.D., Sung, C.-M., Debouck, C., Richardson, S., Levy, M.A., DeWolf, W.E., Jr., Keller, P.M., Tomaszek, T., Head, M.S., Ryan, M.D., Haltiwanger, R.C., Liang, P.-H., Janson, C.A., McDevitt, P.J., Johanson, K., Concha, N.O., Chan, W., Abdel-Meguid, S.S., Badger, A.M., Lark, M.W., Nadeau, D.P., Suva, L.H., Gowen, M., and Nuttall, M.E., *J. Biol. Chem.*, 275(21), (2000) 16007.
- Lee, D., Long, S.A., Murray, J.H., Adams, J.L., Nadeau, D.P., Nuttall, M.E., Kikly, K., Winkler, J.D., Sung, C.-M., Levy, M.A., Keller, P.M., and DeWolf, W.E., *J. Med. Chem.*, 44, (2001) 2015.
- Lee, A., Huang, L., and Ellman, J.A., *J. Am. Chem. Soc.*, 121, (1999) 9907.
- Mjali, A.M.M., Chapman, K.T., Zhao, J., Thornberry, N.A., Peterson, E.P., and MacCoss, M., *Bioorg. Med. Chem. Lett.*, 5, (1995) 317.
- Brady, K.D., Giegel, D.A., Grinnell, C., Lunney, E., Talanian, R.V., Wong, W., and Walker, N., *Bioorg. Med. Chem.*, 7 (1999) 621.
- McMartin, C. and Bohacek, R.S., *J. Comput. Aid. Mol. Des.*, 11, (1997) 333.
- Thompson, L.A. and Ellman, J.A., 'Straightforward and general method for coupling alcohols to solid supports', 9333.
- Dangles, O., Guibe, F., Balavoine, G., Lavielle, S., and Marquet, A., *J. Org. Chem.*, 52, (1987) 4984.
- Carpino, L.A. and El-Faham, A., *Tetrahedron*, 55 (1999) 6813.
- Brady, K.D., *Biochemistry*, 37 (1998) 8508.
- Cleland, W.W., *Meth. Enzymol.*, 63 (1979) 103.